

# Exploring Deep Reinforcement Learning-Assisted Federated Learning for Online Resource Allocation in EdgeIoT

Jingjing Zheng, Kai Li, *Senior Member, IEEE*, Naram Mhaisen, Wei Ni, *Senior Member, IEEE*, Eduardo Tovar, and Mohsen Guizani, *Fellow, IEEE*,

**Abstract**—Federated learning (FL) has been increasingly considered to preserve data training privacy from eavesdropping attacks in mobile edge computing-based Internet of Thing (EdgeIoT). On the one hand, the learning accuracy of FL can be improved by selecting the IoT devices with large datasets for training, which gives rise to a higher energy consumption. On the other hand, the energy consumption can be reduced by selecting the IoT devices with small datasets for FL, resulting in a falling learning accuracy. In this paper, we formulate a new resource allocation problem for EdgeIoT to balance the learning accuracy of FL and the energy consumption of the IoT device. We propose a new federated learning-enabled twin-delayed deep deterministic policy gradient (FL-DLT3) framework to achieve the optimal accuracy and energy balance in a continuous domain. Furthermore, long short term memory (LSTM) is leveraged in FL-DLT3 to predict the time-varying network state while FL-DLT3 is trained to select the IoT devices and allocate the transmit power. Numerical results demonstrate that the proposed FL-DLT3 achieves fast convergence (less than 100 iterations) while the FL accuracy-to-energy consumption ratio is improved by 51.8% compared to existing state-of-the-art benchmark.

**Index Terms**—Federated learning, online resource allocation, deep reinforcement learning, mobile edge computing, Internet of Things.

## I. INTRODUCTION

Mobile edge computing (MEC) provides a promising solution to enabling cloud computing services in mobile edge computing-based Internet of Thing (EdgeIoT) [1], [2]. The IoT devices can offload their local computation-intensive tasks to computationally powerful edge servers [3], [4]. In EdgeIoT, offloading the source data of the IoT devices to the edge server is vulnerable to eavesdropping attacks [5], [6]. To prevent private data leakage of the IoT devices, federated learning (FL) [7] is used to train a global data learning model at the edge server by aggregating the data structure parameters of the IoT devices, while the source data remains at the IoT devices.

Z. Jingjing, K. Li and E. Tovar are with Real-Time and Embedded Computing Systems Research Centre (CISTER), 4249-015 Porto, Portugal (E-mail: {zheng,kai,emt}@isep.ipp.pt).

Naram Mhaisen is with the college of Electrical Engineering, Mathematics, and Computer Science (EEMCS), TU Delft, The Netherlands (e-mail: n.mhaisen@tudelft.nl).

Wei Ni is with the Commonwealth Scientific and Industrial Research Organisation (CSIRO), Sydney 2122, Australia (E-mail: wei.ni@data61.csiro.au).

Mohsen Guizani is with College of Engineering, Qatar University, Doha, Qatar (E-mail: mguizani@ieee.org).

Fig. 1 depicts an FL-enabled EdgeIoT, where the IoT devices are deployed to sense and process private information, e.g., health reports of patients [8]. A local FL model is trained with sensory data at the IoT device. Next, the edge server aggregates the data structure parameters of the local FL models, without collecting the private data of the IoT devices. A global FL model is obtained at the edge server, e.g., by applying FedAvg [9] to the local FL models. The edge server broadcasts the global model back to all the IoT devices. According to the global model, each of the IoT devices renews the training of its local FL model. By iteratively training the local model at the IoT device and updating the global model at the edge server, the learning accuracy of FL on the data classification and event prediction can be progressively improved [10].

On the one hand, selecting the IoT device with large training datasets can improve the learning accuracy of FL [11]. Training the local FL model with large datasets requires numerous CPU cycles and results in high energy consumption, which shortens lifetime of the IoT device. On the other hand, selecting the IoT device with small data for training the local FL model needss a small amount of CPU cycles, which can save the battery energy of the IoT device. However, insufficient training data can lower the learning accuracy of the local FL model and, in turn, reducing the accuracy of the global FL model. Moreover, selecting the IoT device with poor channel quality to offload the local FL model results in a large energy consumption of the IoT device due to frequent retransmissions of local FL models. Therefore, balancing the learning accuracy of FL and energy consumption of the IoT devices is crucial to EdgeIoT.

Moreover, the FL process is time-slotted by design and sequential decision making is required. Hence, in this paper, we propose an online resource allocation optimization to balance the learning accuracy of FL and energy consumption of the IoT devices. In practice, the instantaneous information of data size, transmit power, and link qualities between the edge server and the IoT devices is unlikely to be known. The optimization is formulated as a partially observable Markov decision process (POMDP), where the network state consists of the source data size of the IoT devices, channel conditions between the edge server and the IoT devices, bandwidth and remaining energy of the selected IoT devices. Due to a large and continuous state

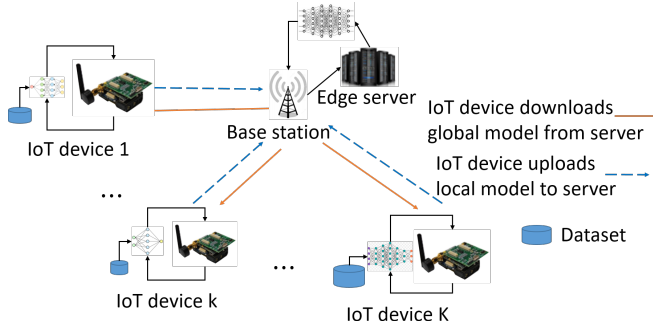


Fig. 1: FL-enabled EdgeIoT. A local FL model is trained with the dataset at the IoT device. The local model is aggregated by an edge server, where the global FL model is trained and returned to the IoT devices.

and action space in the formulated POMDP, a new deep reinforcement learning-based device selection and transmit power allocation algorithm is proposed to maximize the ratio of the learning accuracy of FL and the energy consumption of the IoT devices. The major contributions of this article are summarized as follows:

- The selection of the IoT devices for FL and the allocation of their transmit powers are jointly optimized to balance the learning accuracy of FL and the energy consumption of the IoT devices. Moreover, the proposed optimization is subject to the bandwidth, the training time, the learning accuracy of FL, and the battery budget of the IoT devices.
- Given the large state and action space, FL-DLT3 is proposed to learn the network state dynamics while maximizing the ratio of the learning accuracy of FL to the energy consumption of the IoT devices in real-time. Since the resource allocation for FL is conducted in the continuous domain, the proposed FL-DLT3 is developed based on Twin Delayed Deep Deterministic Policy Gradient (TD3) to optimize the actions of the edge server, i.e., selection of the IoT devices for data collection as well as the transmit power allocation of the selected IoT devices.
- To accelerate the convergence of FL, a new long short term memory (LSTM) layer is developed with the proposed FL-DLT3 to predict the time-varying network states, e.g., data size, bandwidth, channel gain, and remaining energy of the IoT devices. The LSTM layer estimates the unobserved states at every training iteration of the TD3. To the best of our knowledge, this is the first time to employ LSTM with TD3 for the resource allocation of FL-enabled EdgeIoT.
- FL-DLT3 is implemented in PyTorch. The effectiveness of FL-DLT3 is validated with the experimental data. Numerical results show that FL-DLT3 achieves fast convergence (less than 100 iterations) while the FL-accuracy-to-energy-consumption ratio is improved by 51.8%, as compared to the state of the art.

The rest of this paper is structured as follows. The literature on FL-based resource allocation in MEC is reviewed in

Section II. Section III presents the FL protocol and system models. The resource allocation optimization for EdgeIoT is formulated in Section IV. Section V proposes the FL-DLT3 framework which conducts deep reinforcement learning (DRL) based EdgeIoT devices selection and resource allocation. Section VI evaluates the proposed FL-DLT3 framework. Finally, Section VII concludes this paper.

## II. RELATED WORK

This section presents the literature on resource allocation with FL in MEC.

Assuming that the IoT devices have the same computational resources and wireless channel conditions, Federated averaging (FedAvg) [9] randomly selects IoT devices to participate FL training and synchronously aggregates local FL models. This process is repeated until a desirable training accuracy is achieved. In [12], different IoT devices own different computing capabilities and wireless channel conditions, resulting in different local model training time and upload time. The authors develop a FL protocol called FedCS, which allows the server to aggregate as many local model updates as possible to improve image classification accuracy.

To improve the training accuracy of FL systems in the context of wireless channels and energy arrivals of mobile devices, the authors [13] model the transmission power allocation and mobile device selection of the FL training as a constrained Markov decision process. Due to a high complexity, stochastic learning methods and Lagrange multipliers are used to simplify the model and to obtain an efficient policy for all mobile device. In [14], the devices with limited battery energy, CPU computations, and bandwidths, are considered in a mobile crowd network. A deep Q-learning-based resource allocation for data, energy, and CPU cycles is developed to reduce the energy consumption of FL-based mobile devices and training time of the FL. In [15], users are selected for FL training to improve the FL accuracy and reduce the training time and energy consumption of the users. The authors study the user scheduling policy, the CPU-cycle frequency allocated for the training local data and transmit power allocation to balance a fair user scheduling, the accuracy of FL, training time, and energy consumption of users. Given limited computation and communication resources at the devices, [16] analyzes the convergence bound of distributed gradient descent. A control algorithm is developed to determine the tradeoff between local update and global parameter aggregation. Some clients have limited communication and computing resources and fail to complete training tasks, which leads to many discarded learning rounds affecting the model accuracy [17]. The authors study multicriteria-based approach for client selection in FL that reducing the number of communication rounds to reach the intended accuracy and increasing the number of selected clients in each round.

The authors [18] study a trial-and-error based client selection based on multi-armed bandit (MAB), where computation tasks, traffic, and link qualities are unknown. The

MAB-based client selection balances the client selection according to the selection frequency and clients' resources. In [19], the client scheduling in MEC is formulated without the clients' channel and computing information. To reduce the training latency, the client scheduling is formulated as a MAB problem, where  $\epsilon$ -greedy is used to reduce the learning accuracy. In [20], the authors develop a MAB-based client scheduling framework to reduce the training latency of FL. Given the known independent and identically distributed (i.i.d.) local data at the clients, an FL-based client scheduling algorithm is designed.

An FL-based device selection optimization is developed in our preliminary work [21] to balance the energy consumption of the user devices and the learning accuracy of FL. The optimization model takes advantage of the a-priori knowledge of the network state information, e.g., data size, bandwidth, and channel gain. Due to NP-hardness of the optimization, an energy efficiency-FL accuracy balancing heuristic algorithm (FedAECS) was presented in [21] to approximate the optimal client selection policy offline. In contrast, this paper considers a practical scenario without the prior information about data size, bandwidth, channel gain, and remaining energy of the IoT devices. Due to a large state and action space, we propose a new FL-DLT3 to balance FL accuracy and energy consumption of the IoT devices online, where LSTM is leveraged to predict the hidden state of the IoT devices as input state of TD3. In addition, we also compare the performance of the proposed FL-DLT3 with the FedAECS in [21].

### III. SYSTEM MODEL

In this section, we study the training protocol and energy model of FL. The notations used in the paper are summarized in Table I.

#### A. FL Protocol with MEC

Fig. 2 depicts the FL protocol, where the global model at the edge server and the local models at the IoT devices are trained in  $T$  rounds. Each FL round is composed of resource request, IoT device selection, global model aggregation, global model download, local model update and upload. The edge server initializes the hyperparameters of the global model, e.g., learning rate, batch size, and the weights of the global model.

- **Resource Request:** The IoT devices send to the edge server the information needed, i.e., data size, for the device selection.
- **IoT Device Selection:** The edge server selects the IoT devices to upload the local FL model for the training of the global model, where the details will be presented in the next section.
- **Global Model Aggregation:** The edge server aggregates the local FL models of the selected IoT devices to produce the global model.
- **Global Model Download:** All the IoT devices download the the global model from the edge server.

TABLE I: The list of key variables defined in system model

Notation	Definition
$K$	The total number of IoT devices
$k$	Index of IoT device
$T$	The total number of the rounds
$t$	Index of the rounds
$D_{t,k}$	IoT device $k$ owns data size
$\mathbf{x}_{ki}$	Input of the FL model
$y_{ki}$	Output of the FL model
$\mathbf{w}$	Weight parameter of FL training
$\beta_{t,k}$	Whether IoT device $k$ is selected
$f_k$	CPU frequency of IoT device $k$
$\zeta_k$	Effective capacitance coefficient
$L$	Number of local iterations of FL training
$E_{t,k}^{cmp}$	Energy consumption for computing $c_k D_{t,k}$ CPU cycles
$E_{t,k}^{cnp}$	Total computation energy at IoT device $k$
$r_{t,k}^{up}$	Achievable uplink transmit rate
$b_{t,k}$	Bandwidth allocated to IoT device $k$ by the server
$P_{t,k}$	IoT device $k$ transmit power
$G_{t,k}$	Uplink channel gain
$r_{t,k}^{down}$	Achievable downlink transmit rate of device $k$
$H_{t,k}$	Downlink channel gain
$P_t^s$	Transmit power of the edge server
$\tau_{t,k}^{down}$	Downloading time of the global model at device $k$
$\mathfrak{S}_d$	Size of the global model
$\tau_{t,k}^{up}$	Transmission time of the local FL model at $t$
$\mathfrak{S}_u$	Size of the local FL model
$E_{t,k}^{up}$	Energy consumption of device $k$ on the local FL model transmission
$E_{t,k}^c$	Total energy consumption of the selected device $k$
$E_{t,k}$	Remaining battery energy of device $k$
$\Delta E_{t,k}$	Amount of harvested energy
$\Delta_t$	Data evenness of selected devices
$\tau_{t,k}$	Completion time of IoT device $k$ in $t$ round
$\mu_k$	System parameter
$\nu$	Constant value

- **Local Model Update and Upload:** The selected IoT devices individually train their local models according to the FL parameters of the global model.

We consider  $K$  number of IoT devices, where  $k \in [1, K]$ . Let  $\mathbf{x}_{ki}$  and  $y_{ki}$  denote the input (e.g., pixels of an image) and the output (e.g., labels of the image) of the FL model, respectively. The dataset of device  $k$  is denoted as  $\mathcal{D}_{t,k} = \{\mathbf{x}_{ki}, y_{ki}\}_{i=1}^{D_{t,k}}$ , where  $D_{t,k}$  is the size of the dataset of device  $k$  in the  $t$ -th round and data sample  $i$  in device  $k$ . Let  $f(\mathbf{w}, \mathbf{x}_{ki}, y_{ki})$  denote the loss function of FL, which captures approximation errors over the input  $\mathbf{x}_{ki}$  and the output  $y_{ki}$ .  $\mathbf{w}$  is the weight parameter of the loss function of the neural network being trained according to the FL procedure. Given  $D_{t,k}$ , the loss function at IoT device  $k$  can be specified as,

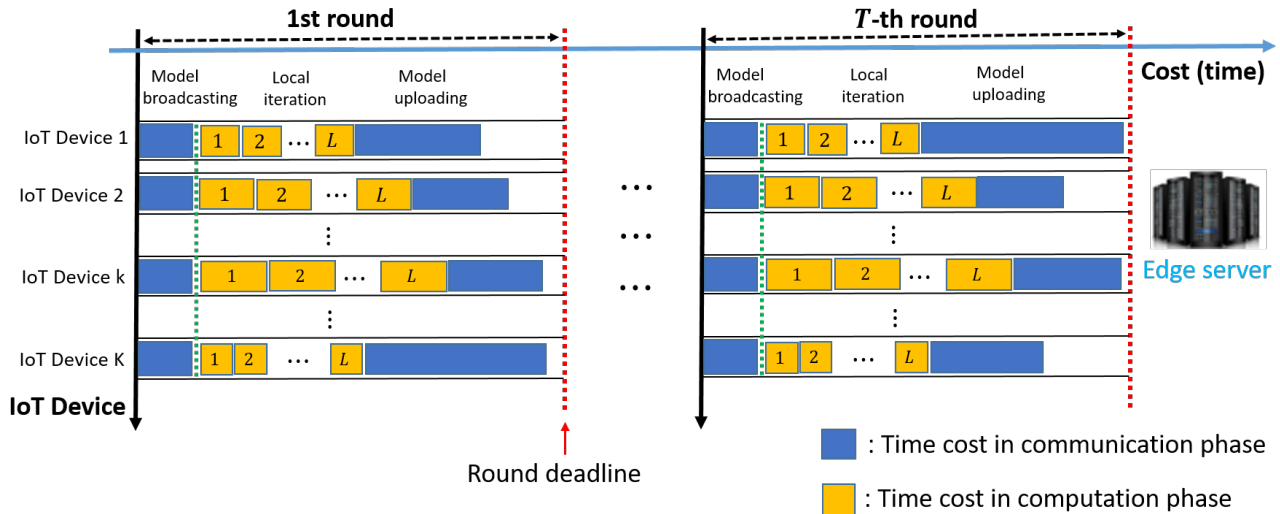


Fig. 2: The whole training process of FL, in each round, the time consumption of IoT device  $k$  includes global model download, local model update and upload.

$$F_{t,k}(\mathbf{w}) = \frac{1}{D_{t,k}} \sum_{i=1}^{D_{t,k}} f(\mathbf{w}, \mathbf{x}_{ki}, y_{ki}). \quad (1)$$

where  $f(\mathbf{w}, \mathbf{x}_{ki}, y_{ki})$  can be specified according to the FL structure. For example,  $f(\mathbf{w}, \mathbf{x}_{ki}, y_{ki}) = \frac{1}{2}(\mathbf{x}_{ki}^T \mathbf{w} - y_{ki})^2$  is used to model linear regression, or  $f(\mathbf{w}, \mathbf{x}_{ki}, y_{ki}) = -\log(1 + \exp(y_{ki} \mathbf{x}_{ki}^T \mathbf{w}))$  is for the model of logistic regression [22]. Since the training of FL aims to minimize the weighted global loss function, we have

$$\begin{aligned} \min_{\mathbf{w}} F_t(\mathbf{w}) &= \sum_{k=1}^K \frac{D_{t,k}}{D_t} F_{t,k}(\mathbf{w}) \\ &= \frac{1}{D_t} \sum_{k=1}^K \sum_{i=1}^{D_{t,k}} f(\mathbf{w}, \mathbf{x}_{ki}, y_{ki}), \end{aligned} \quad (2)$$

where  $D_t = \sum_{k=1}^K D_{t,k}$ , it represents the total the total amount of data in the  $t$ -th round.

### B. Energy Model

The energy consumption of the IoT devices accounts for the local training of the dataset and the transmissions of the local FL model. We assume that training a data sample at the IoT device requires  $c_k$  CPU cycles per bit. Given the data size of  $D_{t,k}$ , the number of CPU cycles for the local model training is  $c_k D_{t,k}$ . We denote  $f_k$  as the computation capacity of IoT device  $k$ , which is measured in CPU cycles per second. According to [23], the computation time of training the local FL model at device  $k$  in the each  $t$ -th round [23], we have

$$\tau_{t,k}^{train} = \frac{L c_k D_{t,k}}{f_k}. \quad (3)$$

According to [24] and [25], the energy consumption on  $c_k D_{t,k}$  CPU cycles at IoT device  $k$  is:

$$E_{t,k1}^{cmp} = \zeta_k c_k D_{t,k} f_k^2, \quad (4)$$

where  $\zeta_k$  is the effective capacitance coefficient of computing chipset for device  $k$ . To compute the local FL model, IoT device  $k$  needs to compute  $c_k D_{t,k}$  CPU cycles with  $L$  is the number of local iterations of FL training. Thus, the total computation energy at IoT device  $k$  in the  $t$ -th round can be given as

$$E_{t,k}^{cmp} = L E_{t,k1}^{cmp} = L \zeta_k c_k D_{t,k} f_k^2 \quad (5)$$

Furthermore, the achievable uplink transmit rate of IoT device  $k$  is given by

$$r_{t,k}^{up} = b_{t,k} \log_2 \left( 1 + \frac{P_{t,k} G_{t,k}}{N_0 b_{t,k}} \right), \quad (6)$$

where  $b_{t,k}$  is the bandwidth allocated to IoT device  $k$  by the edge server in the  $t$ -th round,  $P_{t,k}$  is the power consumption of data transmit for IoT device  $k$ ,  $G_{t,k}$  is the uplink channel gain between device  $k$  and the edge server, and  $N_0$  is the power spectral density of the Gaussian noise.

The achievable downlink transmit rate of device  $k$  is

$$r_{t,k}^{down} = b_{t,k} \log_2 \left( 1 + \frac{P_t^s H_{t,k}}{N_0 b_{t,k}} \right), \quad (7)$$

where  $P_t^s$  denotes the transmit power of the edge server, and  $H_{t,k}$  is the downlink wireless channel gain from the edge server to device  $k$ .

The downloading time of the global model at device  $k$  in the  $t$ -th round is

$$\tau_{t,k}^{down} = \frac{\mathfrak{G}_d}{r_{t,k}^{down}}, \quad (8)$$

where  $\mathfrak{G}_d$  denotes the size of the global model. The transmission time of the local FL model at the  $t$ -th round can be given by

$$\tau_{t,k}^{up} = \frac{\mathfrak{S}_u}{r_{t,k}^{up}}, \quad (9)$$

where  $\mathfrak{S}_u$  is the size of the local FL model. By substituting (6) to (9), the energy consumption of an IoT device on the local FL model transmission is

$$E_{t,k}^{up} = P_{t,k} \tau_{t,k}^{up} = \frac{P_{t,k} \mathfrak{S}_u}{b_{t,k} \log_2 \left( 1 + \frac{P_{t,k} G_{t,k}}{N_0 b_{t,k}} \right)}. \quad (10)$$

The total energy consumption  $E_{t,k}^c$  of the selected IoT device  $k$  in the  $t$ -th round is

$$E_{t,k}^c = E_{t,k}^{cnp} + E_{t,k}^{up} \quad (11)$$

The remaining battery energy of the selected IoT device  $k$  in the  $t$ -th round is

$$E_{t,k} = E_{t-1,k} - E_{t-1,k}^c + \Delta E_{t,k}, \quad (12)$$

where  $\Delta E_{t,k}$  is the amount of harvested energy.

#### IV. PROBLEM FORMULATION

In this section, we study the IoT device selection and transmit power allocation to maximize the ratio of the learning accuracy of FL to the energy consumption of IoT devices.

Let  $\beta_{t,k}$  be a binary indicator. If IoT device  $k$  is selected by the edge server in the  $t$ -th round,  $\beta_{t,k} = 1$ ; otherwise,  $\beta_{t,k} = 0$ . We define the accuracy of FL as the fraction of predictions FL model got right. According to [26]–[28], the accuracy of FL, denoted by  $\Gamma(\beta_{t,k})$ , can be simplified as,

$$\Gamma(\beta_{t,k}) = \log \left( 1 + \sum_{k=1}^K \mu_k \beta_{t,k} D_{t,k} \right) \quad \forall t \in \mathcal{T} \quad (13)$$

where  $\mu_k > 0$  is a system parameter [27]. To improve the evenness of data size of the selected IoT devices, similar to [29], we define the expectation of the difference between the total amount of data for all devices and the amount of data for the selected devices at the  $t$ -th training round, and normalize the expectation, we have,

$$\Delta_t = \frac{\mathbb{E} \left[ \nu \sum_{k=1}^K D_{t,k} - \beta_{t,k} D_{t,k} \right]}{\sum_{k=1}^K D_{t,k}} \quad \forall t \in \mathcal{T}, \quad (14)$$

where  $\nu \in (0, 1]$  is a constant value, the arrival data  $D_{t,k}$  of device  $k$  follows uniform distribution or normal distribution. The objective function can be determined as  $\frac{\Gamma(\beta_{t,k})}{\sum_{k=1}^K \beta_{t,k} E_{t,k}^c} - \Delta_t$ , which aims to balance the learning accuracy of FL and energy consumption of the IoT device and improve the evenness of data size of the selected IoT devices. We formulate the optimization as **P1**.

$$\begin{aligned} \mathbf{P1:} \quad & \max_{\beta_{t,k}, P_{t,k}} \sum_{t=1}^T \left[ \frac{\Gamma(\beta_{t,k})}{\sum_{k=1}^K \beta_{t,k} E_{t,k}^c} - \Delta_t \right] \\ \text{s.t. :} \quad & \beta_{t,k} E_{t,k}^c \leq E_{t,k}, \quad (t \in [1, T], k \in [1, K]) \end{aligned} \quad (15)$$

$$\Gamma(\beta_{t,k}) \geq \epsilon_0, \quad (\epsilon_0 \in (0, 1]) \quad (16)$$

$$\sum_{k=1}^K \beta_{t,k} b_{t,k} \leq B, \quad (t \in [1, T], k \in [1, K]) \quad (17)$$

$$1 \leq \sum_{k=1}^K \beta_{t,k} \leq K, \quad (t \in [1, T], k \in [1, K]) \quad (18)$$

$$\beta_{t,k} \tau_{t,k} \leq t_d, \quad (t \in [1, T], k \in [1, K]) \quad (19)$$

$$P_k^{min} \leq P_{t,k} \leq P_k^{max}, \quad (t \in [1, T], k \in [1, K]) \quad (20)$$

$$\beta_{t,k} \in \{0, 1\}, \quad (t \in [1, T], k \in [1, K]) \quad (21)$$

Specifically,

- Constraint  $(\beta_{t,k} E_{t,k}^c \leq E_{t,k})$  guarantees that the selected IoT device has sufficient energy to complete the local FL model training in  $t$ .
- Constraint  $(\Gamma(\beta_{t,k}) \geq \epsilon_0)$  specifies the minimum requirement of the FL accuracy in  $t$ , where  $\epsilon_0 \in (0, 1]$  defines the lower bound threshold.
- Constraint  $(\sum_{k=1}^K \beta_{t,k} b_{t,k} \leq B)$  guarantees that the total bandwidth of the selected IoT devices is smaller than the bandwidth capacity  $B$ .
- Constraint  $(1 \leq \sum_{k=1}^K \beta_{t,k} \leq K)$  describes that at least one IoT device is selected for FL.
- Constraint  $(\beta_{t,k} \tau_{t,k} \leq t_d)$  ensures that the download, computation and transmit delay of the selected device has to be less than the duration of the round  $t_d$ . As shown in Fig. 2, the each  $t$ -th round contains the downloading time of the global FL model, and local computation and transmission time of the local FL model. According to (3), (8), and (9), we can obtain the time delay  $\tau_{t,k}$ , i.e.,  $\tau_{t,k} = \tau_{t,k}^{train} + \tau_{t,k}^{up} + \tau_{t,k}^{down}$ . Note that the IoT device selection time and training time of the global FL model at the edge server can be neglected since the edge server supports more powerful CPUs than the IoT device.
- Constraint  $(P_k^{min} \leq P_{t,k} \leq P_k^{max})$  indicates the upper and lower bounds of IoT devices' transmit power.

Problem **P1** involves nonlinear problems with continuous and integer variables [30]. The typical 0-1 Multidimensional Knapsack Problem (MKP) [31] is a special case of problem **P1**. Assume that transmit power is a constant, that is, the only variable is the IoT device selection. The items to be put in the knapsack are the IoT devices with energy consumption  $E_{t,k}$ , data size  $D_{t,k}$ , and bandwidth  $b_{t,k}$ . The capacity of the knapsack is equal to the total bandwidth, the variable  $\beta_{t,k}$  is a binary indicator of item (IoT device)  $k$ .  $\beta_{t,k}$  is set to 1 to indicate that item  $k$  is selected. Otherwise,  $\beta_{t,k}$  is set to 0. The total reliability of the knapsack has lower bounds which are equal to the minimum requirement of accuracy constraint (16). Note that every item to be put into the knapsack must obey the time constraint (19).

Coupled with the energy consumption of IoT devices on the transmission is a non-linear function of the transmit power, which has a continuous variable. Therefore, the proposed optimization is NP-hard. It is also mentioning that problem **P1** involves a long time horizon with random and unpredictable data and energy arrivals. This leads to an intractable large state space of the problem require online optimization of selection and allocation decisions.

## V. DRL-BASED IOT DEVICES SELECTION AND RESOURCE ALLOCATION

### A. POMDP Formulation for FL-based IoT Device Selection and Resource Allocation

In this section, the resource allocation is formulated as a POMDP [32].

#### B. State and Action Space

Based on (5) and (10), (15) related to data size  $D_{t,k}$ , transmit power  $P_{t,k}$ , uplink channel gains  $G_{t,k}$ , bandwidth  $b_{t,k}$ , remaining energy of the IoT devices  $E_{t,k}$  and binary indicator  $\beta_{t,k}$  in the each  $t$ -th round. Based on (13), (16) related to  $\beta_{t,k}$  and  $D_{t,k}$ . (17) related to  $\beta_{t,k}$  and  $b_{t,k}$ . (18) only related to  $\beta_{t,k}$ . (19) related to  $D_{t,k}$ ,  $b_{t,k}$ ,  $G_{t,k}$ ,  $H_{t,k}$ ,  $P_{t,k}$  and  $\beta_{t,k}$ . Therefore, the state space of the POMDP consists of data size, uplink channel gains, downlink channel gains, bandwidth and remaining energy of the IoT devices. The network state  $S_\alpha$  is defined as

$$S_\alpha = \{(D_{\alpha,k}, G_{\alpha,k}, H_{\alpha,k}, b_{\alpha,k}, E_{\alpha,k}), k = 1, \dots, K\}. \quad (22)$$

The action in POMDP is the selection of IoT devices for FL, denoted by  $\beta_{\alpha,k}$ , for FL and transmit power allocation  $P_{\alpha,k}$ , which defines

$$\mathcal{A} \in \{(\beta_{\alpha,k}, P_{\alpha,k}), k = 1, \dots, K\}, \quad (23)$$

where  $\beta_{\alpha,k} \in \{0, 1\}$  and  $P_{\alpha,k} \in [P_k^{\min}, P_k^{\max}]$ .

#### C. Observation Space

At state  $S_\alpha$ , the edge server only can get the observation from the state when it selects the IoT devices, and is unable to know the state information of unselected IoT devices. The observation state  $S_\alpha^o \in S_\alpha$  is given by

$$S_\alpha^o = \{(D_{\alpha,k}, G_{\alpha,k}, H_{\alpha,k}, b_{\alpha,k}, E_{\alpha,k})_o, k = 1, \dots, K\}. \quad (24)$$

#### D. Rewards

Let  $S_\alpha^o \times \mathcal{A} \rightarrow \mathcal{R}$  denote the immediate reward received when the action  $A_\alpha \in \mathcal{A}$  is taken. The reward, also named AE gain, is defined as the ratio of FL accuracy and energy consumption of the selected IoT devices adds the term of data evenness of selected devices, i.e.,

$$R(S_\alpha^o | S_\alpha^o, A_\alpha) = \frac{\Gamma(\beta_{\alpha,k})}{\sum_{k=1}^K \beta_{\alpha,k} E_{\alpha,k}^c} - \Delta_\alpha, \quad (25)$$

where  $R(S_\alpha^o | S_\alpha^o, A_\alpha)$  indicates the state observation transits to subsequent  $S_\alpha^o$  from current state  $S_\alpha^o$ . For the sake of simplicity, we use  $R_\alpha$ , instead of  $R(S_\alpha^o | S_\alpha^o, A_\alpha)$ , in the following sections.

To evaluate the action selected by a policy  $\pi_\theta$  with parameters  $\theta$ , where  $\pi_\theta$  is a mapping from state observations to actions, and the set of all policies is defined as  $\Pi$ . We aim to maximize the expected total reward denoted as action-value function  $Q_{\pi_\theta}(S_\alpha^o, A_\alpha)$ ,

$$Q_{\pi_\theta}(S_\alpha^o, A_\alpha) = \max_{\pi \in \Pi} \mathbb{E}_{S_\alpha^o}^{\pi_\theta} \left\{ \sum_{n=0}^{\infty} \gamma^n R_\alpha \right\}, \quad (26)$$

where  $\gamma \in [0, 1]$  is a discount factor for future state observations.  $\mathbb{E}_{S_\alpha^o}^{\pi_\theta} \{\cdot\}$  takes the expectation with respect to policy  $\pi_\theta$  and state observation  $S_\alpha^o$ . According to the Bellman equation [33], the optimal action-value function (26) of a state-action pair  $(S_\alpha^o, A_\alpha)$  and the value of the subsequent state-action pair  $(S_\alpha^o, A_\alpha')$  can be further rewritten as

$$Q_{\pi_\theta}(S_\alpha^o, A_\alpha) = \max_{\pi_\theta \in \Pi} \mathbb{E}_{S_\alpha^o}^{\pi_\theta} \left\{ R_\alpha + \gamma Q_{\pi_\theta}(S_\alpha^o, A_\alpha') \right\}. \quad (27)$$

The optimal action, namely,  $A_\alpha^*$ , which satisfies (27), can be given by

$$A_\alpha^* = \arg \max_{\pi_\theta \in \Pi} \mathbb{E}_{S_\alpha^o}^{\pi_\theta} \left\{ R_\alpha + \gamma Q_{\pi_\theta}(S_\alpha^o, A_\alpha') \right\}, \quad (28)$$

where  $A_\alpha^*$  provides the maximized AE gain.

Given a practical scenario where the edge server has no prior knowledge on the transition probabilities, we propose a FL-DLT3 framework that joint IoT device selection and transmit power allocation algorithm that utilizes TD3, one of the deep reinforcement learning techniques, to maximize the AE gain.

The state and action space increases dramatically with the number of devices, and the action space has both continuous and discrete actions. Moreover, the network state, in practice, is not always observable at the edge server because the data size and remaining energy information of IoT devices are always kept locally before the server takes the devices selection. In view of these challenges, it is difficult to find the exact solution of **P1**. To this end, we develop FL-DLT3 framework to find the near optimal solution of problem **P1**.

In general, FL-DLT3 consists of the TD3-based deep reinforcement learning and the LSTM-based state characterization layer, as depicted in Fig. 3. FL-DLT3 leverages the actor-critic neural network structure to develop the TD3-based deep reinforcement learning [34]. The TD3 at the edge server is trained to optimize IoT device selection and transmit power allocation in a continuous action space, where the edge server has no priori information on the state transition probabilities. The LSTM is used to predict the hidden state of the IoT devices as input state of TD3. The AE gain is maximized over the large continuous state and action spaces.

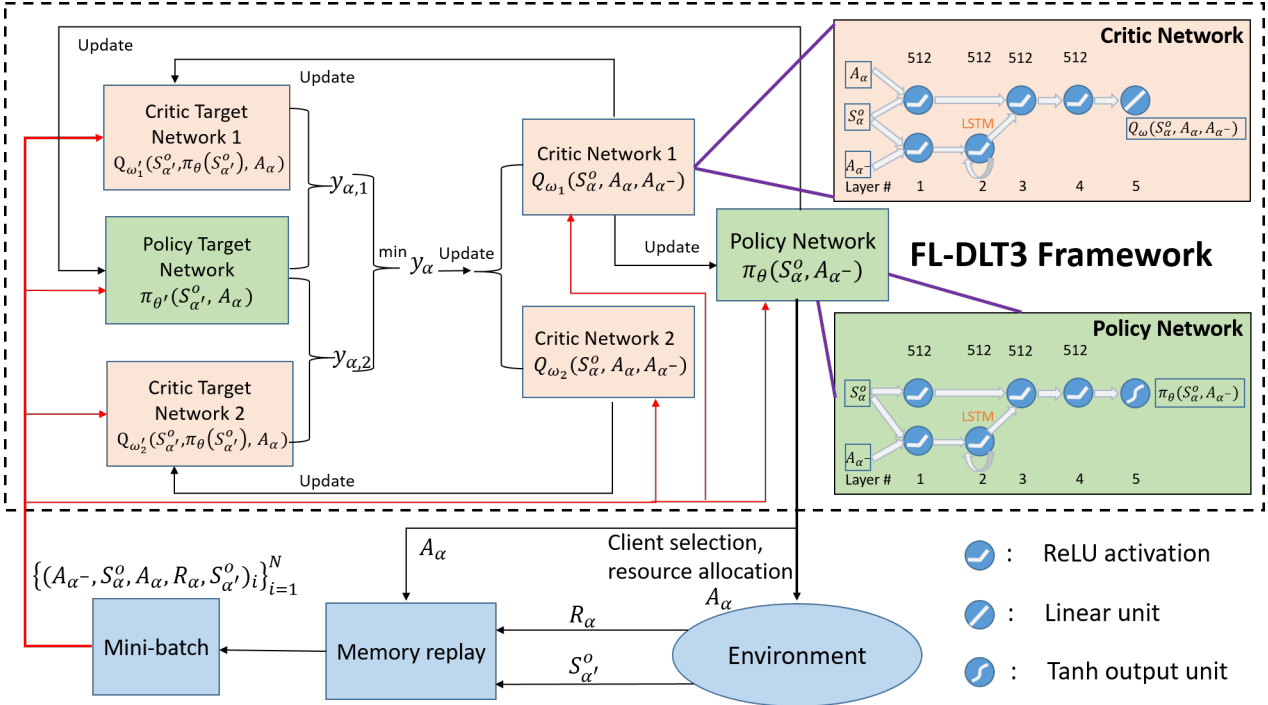


Fig. 3: The proposed FL-DLT3 framework

#### E. TD3 on the Edge Server

TD3 utilizes the deterministic policy gradient algorithm (DPG) [35] to optimally update the current policy by deterministically mapping network states to a specific action of the edge server. The critic is used to approximate the action-value function, which is related to the update of the actor, also known as policy. Moreover, the edge server stores the transition about previous actions of the edge server, current observation, actions of the edge server, AE gain, next observations, i.e.,  $(A_{\alpha-}, S_{\alpha}^o, A_{\alpha}, R_{\alpha}, S_{\alpha'}^o)$ , into the replay buffer  $\mathcal{B}$  at each training step. A mini-batch of  $N$  transitions are randomly sampled from  $\mathcal{B}$  to train the actor-critic networks. The action will be selected according to the policy network with exploration noise after the first  $M$  time steps. Since the IoT device selection action output from the policy network may not be binary, we classify them as binary by setting thresholds. Based on the TD3 framework, the actor and critic networks can be trained to approximate the optimal policy of the formulated POMDP problem.

For the continuous IoT device selection and transmit power allocation, the objective is to find the optimal policy  $\pi_{\theta}$ , which maximizes the expected AE gain  $J(\theta) = \mathbb{E}_{S_{\alpha}^o}^{\pi_{\theta}} [R(S_{\alpha}^o, A_0)]$ , the parametrized policies  $\pi_{\theta}$  can be updated by taking the gradient of the expected return with respect to  $\theta$ , i.e.,

$$\nabla_{\theta} J(\theta) = \mathbb{E}_{\pi_{\theta}} [\nabla_{A_{\alpha}} Q_{\pi_{\theta}}(S_{\alpha}^o, A_{\alpha})|_{A_{\alpha}=\pi(S_{\alpha}^o)} \nabla_{\theta} \pi_{\theta}(S_{\alpha}^o)], \quad (29)$$

where the optimal action-value function can be approximated by the critic neural network [36]  $Q_{\omega}(S_{\alpha}^o, A_{\alpha})$  with parameters  $\omega$ , which obtains the AE gain. To update  $Q_{\omega}(S_{\alpha}^o, A_{\alpha})$ , the critic neural network minimizes the

approximation loss between the current target value and  $Q_{\omega}(S_{\alpha}^o, A_{\alpha})$  by adjusting the parameter  $\omega$ ,

$$\min_{\omega} \mathbb{E} \left[ \left( R_{\alpha} + \gamma Q_{\omega'}(S_{\alpha'}^o, \pi_{\theta}(S_{\alpha'}^o)) - Q_{\omega}(S_{\alpha}^o, A_{\alpha}) \right)^2 \right], \quad (30)$$

where  $\omega'$  stands for the periodically updated parameters of the critic target network,  $\pi_{\theta}(S_{\alpha'}^o)$  is the policy target network takes action in the next state observation  $S_{\alpha'}^o$ .

However, the update of the critic neural network with the above value function may result in overestimation, which can produce suboptimal policies of the policy network. To deal with the overestimation bias problem, TD3 uses two approximately independent critic networks  $\{Q_{\omega_1}, Q_{\omega_2}\}$  to estimate the value function, i.e.,

$$\begin{aligned} y_{\alpha,1} &= R_{\alpha} + \gamma Q_{\omega_1}(S_{\alpha'}^o, \pi_{\theta}(S_{\alpha'}^o)), \\ y_{\alpha,2} &= R_{\alpha} + \gamma Q_{\omega_2}(S_{\alpha'}^o, \pi_{\theta}(S_{\alpha'}^o)), \end{aligned} \quad (31)$$

where the minimum of the two estimators is utilized in the update of the value function, i.e.,  $y_{\alpha} = \min\{y_{\alpha,1}, y_{\alpha,2}\}$ .

Moreover, FL-DLT3 follows TD3 to update the policy and targets less frequently than the Q functions. Delayed policy updates consists of only updating the actor and critic target network every  $d$  intervals. And we also add noise to the target action, which makes the policy network less likely to exploit actions with high Q-value estimates. The proposed FL-DLT3 IoT device selection and transmit power allocation policy is shown in Algorithm 1.

#### F. Network Architecture

Each network follows two-branch structure as in [37], which consists of a feedforward branch and recurrent

branch (as shown in Fig. 3). The feedforward branch and recurrent branch both use five fully-connected layers neural network of 512 hidden nodes. The recurrent branch consists of an embedding layer of 512 fully connected units followed by 512 LSTM units. For each hidden layer (apart from the LSTM), ReLU activations are used between the two hidden layers for both the actor and critic. The final tanh unit and linear unit following the output of the actor and critic, respectively.

### G. LSTM Layer

The unknown network observation transitions resulting from time-varying data size channel gains, data size, bandwidth, and energy harvesting, which increase learning uncertainties, and reduce learning accuracy. The edge server running the FL-DLT3 cannot observe the complete states of all the IoT devices. It can only make the observation of a IoT device when the device is selected and uploads its state information to the edge server. the learning efficiency and accuracy of the TD3-based FL-DLT3 can be compromised by the imperfect knowledge of the states of the IoT devices. Motivated by this fact, we develop a state characterization layer to predict the states of the IoT devices which are not observable, and feed the predicted states into the every neural network of FL-DLT3.

For every policy (target) network, two critic (target) networks and memory replay, we use LSTM to predict their respective hidden states. At time state  $i$ , the hidden states  $h_i^{hid}$  is calculated by the following composite function

$$h_i^{hid} = o_i \tanh(C_i) \quad (32)$$

$$o_i = \sigma(W_0 \cdot [C_i, h_{i-1}^{hid}, A_i] + e_0) \quad (33)$$

$$C_i = F_i C_{i-1} + p_i \tanh(W_c \cdot [h_{i-1}^{hid}, A_i] + e_c) \quad (34)$$

$$F_i = \sigma(W_f \cdot [h_{i-1}^{hid}, C_{i-1}, A_i] + e_f) \quad (35)$$

$$p_i = \sigma(W_p \cdot [h_{i-1}^{hid}, C_{i-1}, A_i] + e_p) \quad (36)$$

where  $o_i$ ,  $C_i$ ,  $F_i$ , and  $p_i$  denote the output gate, cell activation vectors, forget gate, and input gate of the LSTM layer, respectively.  $\sigma$ , and  $\tanh$  refer to logistic sigmoid function and the hyperbolic tangent function, respectively.  $\{W_0, W_c, W_f, W_p\}$  are the weight matrix, and  $\{e_0, e_c, e_f, e_p\}$  are the bias matrix.

## VI. NUMERICAL EXPERIMENTS

In this section, we present the implementation of the proposed FL-DLT3 on PyTorch, which is an open source machine learning library based on the Torch library. We compare FL-DLT3 with benchmarks in terms of network size, data size, and communication bandwidth. Table II specifies the configuration of simulation parameters.

---

### Algorithm 1 The developed FL-DLT3 IoT device selection and resource allocation policy

---

- 1: Initialize critic networks  $\{Q_{\omega_1}(S_{\alpha}^o, A_{\alpha}, A_{\alpha-}), Q_{\omega_2}(S_{\alpha}^o, A_{\alpha}, A_{\alpha-})\}$  and actor network  $\pi_{\theta}(S_{\alpha}^o, A_{\alpha-})$  with random parameters  $\omega_1, \omega_2, \theta$ .
- 2: Initialize target networks  $\omega'_1 \leftarrow \omega_1, \omega'_2 \leftarrow \omega_2, \theta' \leftarrow \theta$ .
- 3: Initialize environment  $S_{\alpha}^o$ , past actions  $A_{\alpha-} \leftarrow \mathbf{0}$ , relay buffer  $\mathcal{B}$
- 4: **for**  $\alpha = 1, \dots, T$  **do**
- 5:   Select action with exploration noise  $A_{\alpha} \sim \pi_{\theta}(S_{\alpha}^o, A_{\alpha-}) + \rho, \rho \sim \mathcal{N}(0, \sigma)$ .
- 6:   Server allocates the selected IoT devices  $P_{\alpha, k}$
- 7:   Server performs model aggregation to obtain updated global model and distributes it to all selected clients in the next epoch.
- 8:   Server observes new observation  $S_{\alpha}'^o$ , calculates  $R_{\alpha}$ , and stores the experience  $(A_{\alpha-}, S_{\alpha}^o, A_{\alpha}, R_{\alpha}, S_{\alpha}'^o)$  into  $\mathcal{B}$
- 9:   Sample mini-batch of  $N$  experiences  $\{(A_{\alpha-}, S_{\alpha}^o, A_{\alpha}, R_{\alpha}, S_{\alpha}'^o)_i\}_{i=1}^N$  from  $\mathcal{B}$
- 10:   Obtain target action  $A_{\alpha'} \leftarrow \pi_{\theta'}(S_{\alpha'}^o, A_{\alpha}) + \hat{\rho}, \hat{\rho} \sim \text{Clip}(\mathcal{N}(0, \hat{\sigma}), -c, c)$
- 11:    $\hat{y} \leftarrow R_{\alpha} + \gamma \min_{m=1,2} Q_{\omega_m}(S_{\alpha'}^o, \hat{A}_{\alpha'}, A_{\alpha})$  update critics  $\omega_m \leftarrow \arg \min_{\omega_m} \mathbb{E}(\hat{y} - Q_{\omega_m}(S_{\alpha}^o, A_{\alpha-}))^2$
- 12:   **if**  $\alpha \bmod d = 0$  **then**
- 13:     Update  $\theta$  by the deterministic policy gradient using equation (29).
- 14:     Update target networks:
- 15:      $\omega_m' \leftarrow \varphi \omega_m + (1 - \varphi) \omega_m'$
- 16:      $\theta' \leftarrow \varphi \theta + (1 - \varphi) \theta'$
- 17:   **end if**
- 18: **end for**

---

### A. Implementation and Training of FL-DLT3

We implement the proposed FL-DLT3 with Python 3.9. Pytorch is set up on a Linux workstation with 64-bit Ubuntu 18.04. FL-DLT3 trains the resource allocation with FL on 2 Nvidia's GPUs, one is GeForce GTX 1060 with 3 GB memory, the other is GeForce RTX 2060 with 6 GB memory.

The experience replay memory can store  $5 \times 10^5$  training samples in terms of *previous actions of the edge server, current observation, actions of the edge server, AE gain, next observations*. The previous actions and current observation are combined to feed into policy network and critic networks to infer the hidden state. Both state space and action space are updated by using Adam optimizer, where the learning rate is  $3 \times 10^{-4}$ . At one training step, the actor and critic networks are trained with a mini-batch of 45 transitions, sampled from the experience replay memory.

The policy target network is implemented by adding  $\rho \sim \mathcal{N}(0, 0.5)$  to the actions chosen by the actor target network, clipped to  $(0, 60)$ . The delayed policy updates the actor and critic target networks every  $d$  intervals, where  $d = 10$ .

TABLE II: Simulation parameters

Parameters	Values
Number of rounds ( $T$ )	1000
Number of local iterations ( $L$ )	4
For training one data sample	20 cycles / bit
CPU cycles per bit ( $c_k$ )	
Computation capacity of IoT device $k$ ( $f_k$ )	[2, 4] GHZ
Transmit power of IoT device $k$ ( $P_{t,k}$ )	[0.1, 60] W
Transmit power of the edge server ( $P_t^s$ )	[100,1000] W
Uplink channel gain ( $G_{t,k}$ )	[ $10^{-3}, 10^{-1}$ ] dB
Downlink channel gain ( $H_{t,k}$ )	[ $10^{-1}, 10$ ] dB
Power spectral density of the Gaussian noise ( $N_0$ )	$1.0 \times 10^{-8}$
Parameter size of the global model ( $S_d$ )	$1 \times 10^4$ bit
Upload data size of IoT device ( $S_u$ )	$5 \times 10^4$ bit
Binary indicator of device selection ( $\beta_{t,k}$ )	{0, 1}
System parameter ( $\mu_k$ )	$4.2 \times 10^{-9}$
Effective capacitance coefficient ( $\epsilon_k$ )	$1.2 \times 10^{-28}$
The amount of harvested energy ( $\Delta E_{t,k}$ )	[50, 200] J
The constant value ( $\nu$ )	1.0
Critic network learning rate	$3 \times 10^{-4}$
Actor network learning rate	$3 \times 10^{-4}$
Neural network weight coefficient ( $\phi$ )	$5 \times 10^{-3}$
Interval of policy target network update ( $d$ )	10
Discount factor ( $\gamma$ )	0.99
Batch size ( $N$ )	45
Replay buffer size ( $ \mathcal{B} $ )	$5 \times 10^5$
Exploration noise ( $\sigma$ )	0.5
Clipped normal noise ( $c$ )	0.5

### B. AE Gain Performance

For performance validation, we compare FL-DLT3 with existing state-of-the-art FL-based device scheduling approaches, i.e., FedAECS [21], FedCS [12] and FedAvg [9].

- **FedAECS:** the edge server selects the IoT devices to fulfill a predetermined ratio of FL accuracy to energy consumption, while meeting the requirement of accuracy and bandwidth.
- **FedCS:** given the bandwidth limit, the edge server selects the maximum number of IoT devices for FL.
- **FedAvg:** Given the limit of the bandwidth, the edge server determines the number of IoT devices for FL training, and randomly selects the IoT devices.

Fig. 4 shows the AE gains, where the  $t$ -th round is from 1 to 1000 and  $K = 40$ . The data size  $D_{t,k}$  and bandwidth  $b_{t,k}$  of the  $K$  devices vary in [2, 10] MB and [10, 50] KHz, respectively. In general, the proposed FL-DLT3 achieves the highest AE gain, as compared to the existing FedAECS, FedCS, and FedAvg, improved by 51.8%, 82.4% and 85.0% respectively. The reason is that FL-DLT3 leverages experience replay and predict the states of the IoT devices which are not observable, however, FedAECS, FedCS, and FedAvg are unable to predict the states of the IoT devices.

FL-DLT3 outperforms FL-DLT3 without the LSTM layer with a gain of 39.8%. This is because the LSTM layer efficiently predicts the unknown network observation tran-

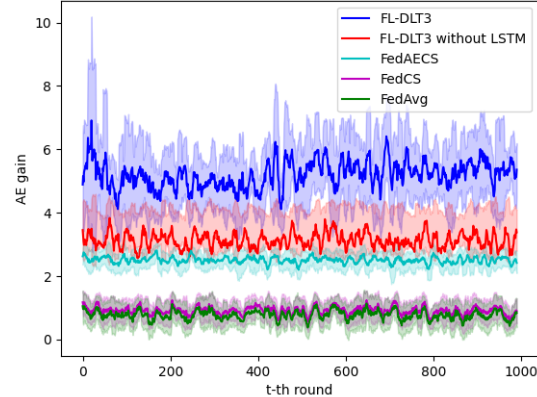


Fig. 4: Comparison of the AE gains, where  $T = 1000$  and  $K = 40$ .

sitions, which enriches the training environment for FL and TD3.

Fig. 5 studies the AE gain of the proposed FL-DLT3, where  $K$  increases from 10 to 80. In general, the proposed FL-DLT3 achieves the highest AE gain 11.4557, as compared to the existing FedAECS ( 2.7212), FedCS ( 1.3952), and FedAvg (1.3498) given  $K = 10$ .

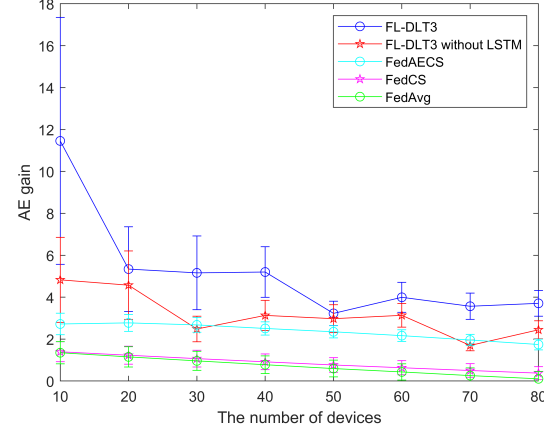


Fig. 5: Comparison of the AE gain obtained by using FL-DLT3, FL-DLT3 without LSTM, FedAECS, FedCS and FedAvg with different number of IoT devices

In Fig. 6, it can be observed that the energy consumption of FL-DLT3 dominates the performance when  $K$  increase from 10 to 50. When  $K > 60$ , the FL accuracy dominates the performance. This confirms that the AE gain's fluctuation in Fig. 5 when  $K$  increase from 10 to 50. The reasons is that FL-DLT3 can select more IoT devices, hence the FL accuracy and energy consumption increase monotonically with the number of devices.

Fig. 7 shows the AE gain given 1000 rounds. With an increase of  $K$ , the AE gain achieved by FL-DLT3 decreases from 5.3411 to 3.7066. This also validates the performance in Fig. 5.

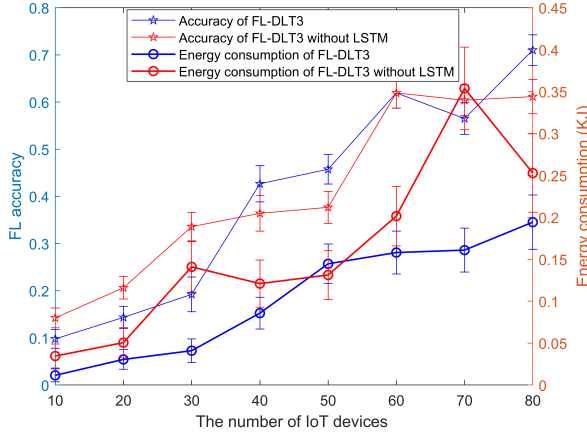


Fig. 6: Compare the FL accuracy and energy consumption of FL-DLT3 and FL-DLT3 without LSTM as the number of devices changes

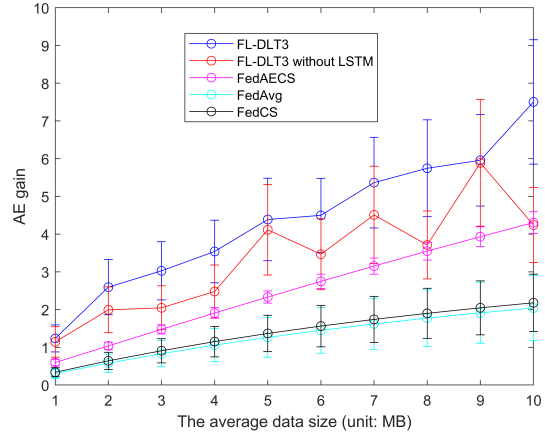


Fig. 8: AE gain varying with data size following normal distribution while keeping the same variance (0.2 MB)

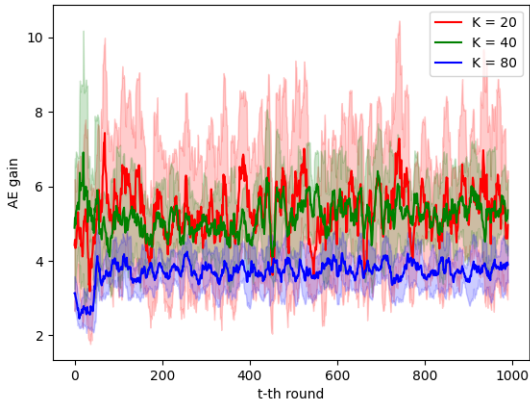


Fig. 7: The AE gain achieved by the proposed FL-DLT3 given  $K = 20, 40$ , or  $80$ .

Fig. 8 depicts the AE gain of FL-DLT3 with regards to the average data size. In general, the AE gain increases with the growth of the data size. This is because the FL accuracy rises in a high rate while the energy consumption of the IoT devices on the training of FL-DLT3 slightly increases. Moreover, the AE gain obtained by FL-DLT3 is about twice that obtained by FedAECS, thanks to the transmit power allocation in FL-DLT3.

Fig. 9 describes the AE gain of FL-DLT3 with regards to the average bandwidth. Overall, the AE gain raises with an increase of the average bandwidth since the energy consumption of the IoT devices on the local FL models transmission is reduced since a better channel quality leads to smaller packet retransmission and energy consumption. In addition, FL-DLT3 achieves the highest AE gain given different bandwidths. This is achieved by the LSTM layer integrated into the FL-DLT3 to predict the time-varying bandwidth.

Fig. 10 shows the FL accuracy and energy consumption of FL-DLT3 and FL-DLT3 without LSTM in regard to the

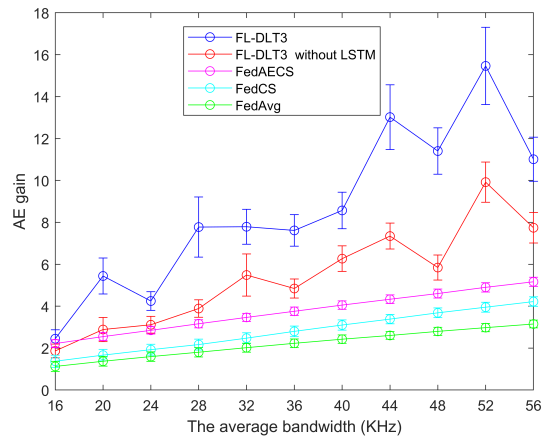


Fig. 9: AE gain varying with bandwidth following normal distribution while keeping the same variance (4 KHz)

average bandwidth size of IoT devices changes. Generally, the energy consumption of FL-DLT3 decreases with an increase of the bandwidth since the retransmission of the local FL models is reduced.

Fig. 11 shows the runtime of FL-DLT3, where  $K$  is set to 10, 40, 60, or 80. In the first 45 rounds, the runtime of FL-DLT3 is about 0.018 s. This is because the experience replay buffer is initialized in which the training of FL-DLT3 is not conducted yet. Once the learning experience is sufficient and FL-DLT3 carries out the training, the runtime raises to 0.74 s given  $K = 10$ . When  $K$  increases to 80, the training of FL-DLT3 takes 1.3286 seconds. The reason is that an increase of the IoT devices results in a large state and action space, hence the learning time of FL-DLT3 increases. In addition, the runtime of FL-DLT3 randomly fluctuates. This is due to random interruptions from other program executions that are concurrently operated on the server.

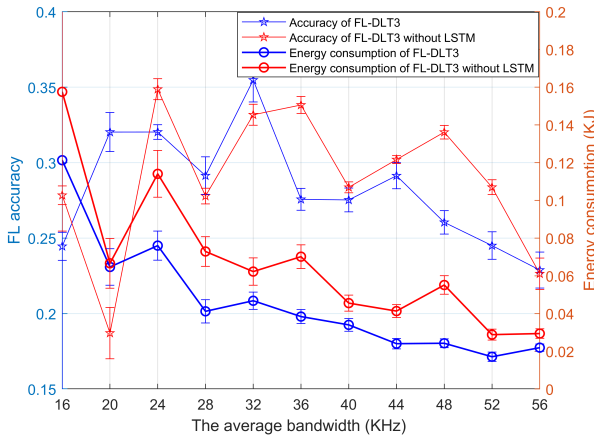


Fig. 10: Compare the FL accuracy and energy consumption of FL-DLT3 and FL-DLT3 without LSTM as the average channel size of IoT devices changes

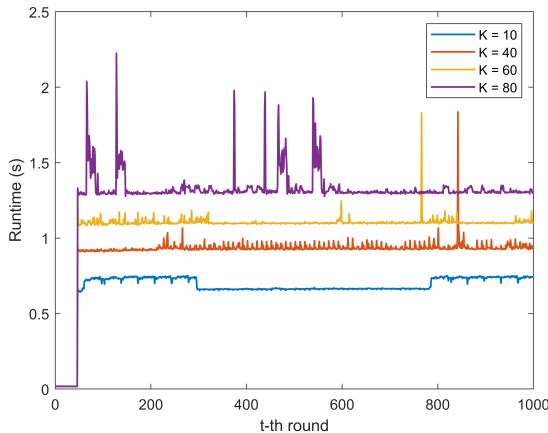


Fig. 11: Runtime with  $t$ -th round

## VII. CONCLUSION

In this paper, we proposed FL-DLT3, which is a new deep reinforcement learning based resource allocation with FL for EdgeIoT. Given the large state and action space, FL-DLT3 learns the network state dynamics while maximizing the ratio of the learning accuracy of FL to the energy consumption of the IoT devices in a continuous domain. To improve the learning accuracy, a new state characterization layer based on LSTM is developed in FL-DLT3 to predict the time-varying data size, bandwidth, channel gain, and remaining energy of the IoT devices. FL-DLT3 is implemented in PyTorch. The effectiveness of FL-DLT3 is validated with the experimental data.

## REFERENCES

- [1] Y. Mao, C. You, J. Zhang, K. Huang, and K. B. Letaief, "A survey on mobile edge computing: The communication perspective," *IEEE Communications Surveys & Tutorials*, vol. 19, no. 4, pp. 2322–2358, 2017.
- [2] X. Sun and N. Ansari, "Edgeiot: Mobile edge computing for the internet of things," *IEEE Communications Magazine*, vol. 54, no. 12, pp. 22–29, 2016.
- [3] P. Mach and Z. Becvar, "Mobile edge computing: A survey on architecture and computation offloading," *IEEE Communications Surveys & Tutorials*, vol. 19, no. 3, pp. 1628–1656, 2017.
- [4] O. A. Wahab, A. Mourad, H. Orok, and T. Taleb, "Federated machine learning: Survey, multi-level classification, desirable criteria and future directions in communication and networking systems," *IEEE Communications Surveys Tutorials*, vol. 23, no. 2, pp. 1342–1397, 2021.
- [5] L. Xiao, X. Wan, C. Dai, X. Du, X. Chen, and M. Guizani, "Security in mobile edge caching with reinforcement learning," *IEEE Wirel. Commun.*, vol. 25, no. 3, pp. 116–122, 2018. [Online]. Available: <https://doi.org/10.1109/MWC.2018.1700291>
- [6] S. A. Rahman, H. Tout, C. Talhi, and A. Mourad, "Internet of things intrusion detection: Centralized, on-device, or federated learning?" *IEEE Network*, vol. 34, no. 6, pp. 310–317, 2020.
- [7] B. McMahan, E. Moore, D. Ramage, S. Hampson, and B. A. y Arcas, "Communication-efficient learning of deep networks from decentralized data," in *Artificial Intelligence and Statistics*. PMLR, 2017, pp. 1273–1282.
- [8] L. Xiao, X. Wan, X. Lu, Y. Zhang, and D. Wu, "IoT security techniques based on machine learning: How do IoT devices use AI to enhance security?" *IEEE Signal Processing Magazine*, vol. 35, no. 5, pp. 41–49, 2018.
- [9] H. B. McMahan, E. Moore, D. Ramage, and B. A. y Arcas, "Federated learning of deep networks using model averaging," *CoRR*, vol. abs/1602.05629, 2016. [Online]. Available: <http://arxiv.org/abs/1602.05629>
- [10] S. Abdulrahman, H. Tout, H. Ould-Slimane, A. Mourad, C. Talhi, and M. Guizani, "A survey on federated learning: The journey from centralized to distributed on-site learning and beyond," *IEEE Internet of Things Journal*, vol. 8, no. 7, pp. 5476–5497, 2021.
- [11] D. C. Verma, S. B. Calo, S. Witherspoon, E. Bertino, A. A. Jabal, A. Swami, G. Cirincione, S. Julier, G. White, G. de Mel, and G. Pearson, "Federated learning for coalition operations," *CoRR*, vol. abs/1910.06799, 2019. [Online]. Available: <http://arxiv.org/abs/1910.06799>
- [12] T. Nishio and R. Yonetani, "Client selection for federated learning with heterogeneous resources in mobile edge," in *ICC 2019 - 2019 IEEE International Conference on Communications (ICC)*, 2019, pp. 1–7.
- [13] S. Chu, J. Li, J. Wang, Z. Wang, M. Ding, Y. Zang, Y. Qian, and W. Chen, "Federated learning over wireless channels: Dynamic resource allocation and task scheduling," *CoRR*, vol. abs/2106.06934, 2021. [Online]. Available: <https://arxiv.org/abs/2106.06934>
- [14] T. T. Anh, N. C. Luong, D. I. Niyato, D. I. Kim, and L. Wang, "Efficient training management for mobile crowd-machine learning: A deep reinforcement learning approach," *IEEE Wirel. Commun. Lett.*, vol. 8, no. 5, pp. 1345–1348, 2019. [Online]. Available: <https://doi.org/10.1109/LWC.2019.2917133>
- [15] B. Yin, Z. Chen, and M. Tao, "Joint user scheduling and resource allocation for federated learning over wireless networks," in *GLOBECOM 2020 - 2020 IEEE Global Communications Conference*, 2020, pp. 1–6.
- [16] S. Wang, T. Tuor, T. Salonidis, K. K. Leung, C. Makaya, T. He, and K. Chan, "Adaptive federated learning in resource constrained edge computing systems," *IEEE Journal on Selected Areas in Communications*, vol. 37, no. 6, pp. 1205–1221, 2019.
- [17] S. Abdulrahman, H. Tout, A. Mourad, and C. Talhi, "Fedmcbs: Multicriteria client selection model for optimal IoT federated learning," *IEEE Internet of Things Journal*, vol. 8, no. 6, pp. 4723–4735, 2021.
- [18] N. Yoshida, T. Nishio, M. Morikura, and K. Yamamoto, "Mab-based client selection for federated learning with uncertain resources in mobile networks," in *2020 IEEE Globecom Workshops (GC Wkshps)*. IEEE, 2020, pp. 1–6.
- [19] B. Xu, W. Xia, J. Zhang, T. Q. Quek, and H. Zhu, "Online client scheduling for fast federated learning," *IEEE Wireless Communications Letters*, 2021.
- [20] W. Xia, T. Q. S. Quek, K. Guo, W. Wen, H. H. Yang, and H. Zhu, "Multi-armed bandit-based client scheduling for federated learning," *IEEE Transactions on Wireless Communications*, vol. 19, no. 11, pp. 7108–7123, 2020.
- [21] J. Zheng, K. Li, E. Tovar, and M. Guizani, "Federated learning for energy-balanced client selection in mobile edge computing," in *2021 International Wireless Communications and Mobile Computing (IWCMC)*. IEEE, 2021, pp. 1942–1947.

- [22] S. Shalev-Shwartz and S. Ben-David, *Understanding machine learning: From theory to algorithms*. Cambridge university press, 2014.
- [23] C. T. Dinh, N. H. Tran, M. N. H. Nguyen, C. S. Hong, W. Bao, A. Y. Zomaya, and V. Gramoli, “Federated learning over wireless networks: Convergence analysis and resource allocation,” *IEEE/ACM Trans. Netw.*, vol. 29, no. 1, p. 398–409, feb 2021. [Online]. Available: <https://doi.org/10.1109/TNET.2020.3035770>
- [24] Z. Yang, M. Chen, W. Saad, C. S. Hong, and M. Shikh-Bahaei, “Energy efficient federated learning over wireless communication networks,” *IEEE Transactions on Wireless Communications*, vol. 20, no. 3, pp. 1935–1949, 2020.
- [25] Y. Mao, J. Zhang, and K. B. Letaief, “Dynamic computation offloading for mobile-edge computing with energy harvesting devices,” *IEEE Journal on Selected Areas in Communications*, vol. 34, no. 12, pp. 3590–3605, 2016.
- [26] Y. Zhan, P. Li, Z. Qu, D. Zeng, and S. Guo, “A learning-based incentive mechanism for federated learning,” *IEEE Internet of Things Journal*, 2020.
- [27] W. Y. B. Lim, J. Huang, Z. Xiong, J. Kang, D. Niyato, X.-S. Hua, C. Leung, and C. Miao, “Towards federated learning in uav-enabled internet of vehicles: A multi-dimensional contract-matching approach,” *IEEE Transactions on Intelligent Transportation Systems*, 2021.
- [28] L. U. Khan, S. R. Pandey, N. H. Tran, W. Saad, Z. Han, M. N. Nguyen, and C. S. Hong, “Federated learning for edge networks: Resource optimization and incentive mechanism,” *IEEE Communications Magazine*, vol. 58, no. 10, pp. 88–93, 2020.
- [29] X. Lyu, C. Ren, W. Ni, H. Tian, R. P. Liu, and E. Dutkiewicz, “Optimal online data partitioning for geo-distributed machine learning in edge of wireless networks,” *IEEE Journal on Selected Areas in Communications*, vol. 37, no. 10, pp. 2393–2406, 2019.
- [30] N. V. Sahinidis, “Mixed-integer nonlinear programming 2018,” 2019.
- [31] H. Kellerer, U. Pferschy, and D. Pisinger, “Multidimensional knapsack problems,” in *Knapsack problems*. Springer, 2004, pp. 235–283.
- [32] L. P. Kaelbling, M. L. Littman, and A. R. Cassandra, “Planning and acting in partially observable stochastic domains,” *Artificial intelligence*, vol. 101, no. 1-2, pp. 99–134, 1998.
- [33] R. Bellman, “Dynamic programming,” *Science*, vol. 153, no. 3731, pp. 34–37, 1966.
- [34] S. Fujimoto, H. Hoof, and D. Meger, “Addressing function approximation error in actor-critic methods,” in *International Conference on Machine Learning*. PMLR, 2018, pp. 1587–1596.
- [35] D. Silver, G. Lever, N. Heess, T. Degris, D. Wierstra, and M. Riedmiller, “Deterministic policy gradient algorithms,” in *International conference on machine learning*. PMLR, 2014, pp. 387–395.
- [36] V. Mnih, K. Kavukcuoglu, D. Silver, A. A. Rusu, J. Veness, M. G. Bellemare, A. Graves, M. Riedmiller, A. K. Fidjeland, G. Ostrovski *et al.*, “Human-level control through deep reinforcement learning,” *nature*, vol. 518, no. 7540, pp. 529–533, 2015.
- [37] X. B. Peng, M. Andrychowicz, W. Zaremba, and P. Abbeel, “Sim-to-real transfer of robotic control with dynamics randomization,” in *2018 IEEE international conference on robotics and automation (ICRA)*. IEEE, 2018, pp. 3803–3810.